

UNLIMITED RELEASE

SC-RR-68-619

ANALYTICAL APPROXIMATIONS FOR TOTAL  
PAIR-PRODUCTION CROSS SECTIONS

Frank Biggs, 5231  
Ruth Lighthill, 5231

September 1968

BEST AVAILABLE COPY

ABSTRACT

Analytical approximations which are efficient for use in computer programs are given for total pair-production cross sections for atomic numbers  $1 \leq Z \leq 100$  in the photon energy interval  $1022.012 \leq E \leq 10^5$  keV. Graphs of cross sections and approximation parameters in tabular form are included.

III

TOTAL PAGES: 22

1-2

## ANALYTICAL APPROXIMATIONS FOR TOTAL PAIR-PRODUCTION CROSS SECTIONS

Whenever x-ray cross sections are needed in computer programs, it is convenient to have approximations for them in analytical form. It is desirable that these analytical expressions exhibit such properties as speed in computer evaluation, economy in memory storage, ease in adapting to composite materials, and as much accuracy as the "source data" justify. The term "source data" is used here to refer to the input data to the curve-fitting programs. A scheme such as this which applies to the photoelectric and Klein-Nishina cross sections is described in detail in an earlier report by the authors.<sup>1</sup> This report gives the results of our efforts to include the total pair production in the scheme.

Pair production is the photon-matter interaction wherein a photon of sufficient energy encounters a strong electric field and is converted into an electron-positron pair. We use the expression "total pair-production cross section" to mean the sum of the cross sections for pair production in the field of the atomic nucleus plus pair production in the fields of the atomic electrons.

The units used are keV (kiloelectron volts) for photon energies and  $\text{cm}^2/\text{gm}$  for the cross sections. The range of atomic numbers considered is  $1 \leq Z \leq 100$  and the photon energy range is from threshold to  $10^5$  keV.

A least squares fitting technique was used to fit the analytical expressions to the source data. The technique has been described in a report by one of the authors.<sup>2</sup>

Source data were taken from Storm and Israel<sup>3</sup> who estimate that the nuclear field cross sections are accurate to within 5 percent and that the electron field cross sections are accurate to within 10 percent.

After preliminary numerical experimentation, it appeared that a suitable function to use as an approximation was

$$\mu(E) = \begin{cases} 0, & E < B \\ C(E - B)^2, & B \leq E \leq 1500 \text{ keV} \\ \frac{1}{1 + 1.7 \times 10^{-13} V^6} \sum_{n=1}^7 A_n V^n, & 1500 \text{ keV} < E \leq 10^5 \text{ keV}, \end{cases} \quad (1)$$

where  $\mu$  is the total pair-production cross section in  $\text{cm}^2/\text{gm}$ ,  $E$  is photon energy in keV,  $V = (E - B)^{1/2}$ ,  $B = 2mc^2 = 1022.012 \text{ keV}$  ( $m$  is electronic mass and  $c$  is speed of light). A set of fitting parameters,  $C$  and  $A_n$ 's, is needed for each element. These are tabulated in the parameter table, Table I, versus the atomic number  $Z$ . Since we require that the function  $\mu$  be continuous at  $E = 1500 \text{ keV}$ , the value of the parameter  $C$  can be calculated from the  $A_n$ 's, but for convenience we give the values of  $C$  in Table I for each element.

Figures 1 through 10 are curves which represent  $\mu$  of Eq. (1) for each element, using the fitting parameters given in Table I. Source data in the graphs are indicated by asterisks. Adjacent curves represent a difference of 10 in atomic number. The atomic number  $Z$  increases in going upward from one curve to the next; the top and bottom curves are labeled by the corresponding values of  $Z$ .

The part of the function of Eq. (1), applying in the interval  $B < E \leq 1500 \text{ keV}$ , was used to provide a smooth extrapolation of the approximation to zero at the nuclear field cross section threshold energy  $E = B$ . Even though the approximation for use in the interval above  $E = 1500 \text{ keV}$  goes to zero at  $E = B$ , it does not always do so in a smooth manner and, indeed, would give negative values for photon energies slightly above  $E = B$  for all the elements that exhibit a negative value for  $A_1$  in Table I.

As a measure of the average relative error involved in fitting Eq. (1) to the source data of each element, we use

$$\epsilon = \left\{ \frac{1}{M} \sum_{i=1}^M \left[ \frac{\mu(E_i) - \hat{\mu}(E_i)}{\hat{\mu}(E_i)} \right]^2 \right\}^{1/2}, \quad (2)$$

where  $\epsilon$  is the rms error,  $M$  is the number of source data cross sections,  $\mu(E_i)$  is Eq. (1) evaluated at  $E = E_i$ , and  $\hat{\mu}(E_i)$  is the source data cross section for photon energy  $E_i$ . The rms error is given for each element in Table I.

It should be noted that the fitting parameters,  $C$  and  $A_n$ 's, are tabulated in Table I to fewer decimal places of accuracy than the computer (CDC 3600) uses. A calculation was made to round off the parameters as much as possible without increasing the rms error by more than 1/2 percent. It is the rounded values that appear in the table. Whenever a parameter is rounded off to less than four significant places, the printout format is such that zeros are printed in the remaining places. The curves of Figs. 1 through 10 and the rms errors of Table I were obtained by using the rounded-off parameters.

For a composite material consisting of  $N$  elements, the approximation for the total pair-production cross sections in  $\text{cm}^2/\text{gm}$  is

$$\mu(E) = \sum_{i=1}^N f_i \mu_i(E) \quad (3)$$

where  $f_i$  is the fraction (by mass) of element  $i$  that occurs in the material and  $\mu_i(E)$  is Eq. (1), applied when the set of fitting parameters corresponding to element  $i$  is used. If one substitutes Eq. (1) into Eq. (3) and interchanges sums,  $\bar{\mu}$  becomes

$$\mu(e) = \begin{cases} 0, & E < B \\ \bar{C} (E - B)^2, & B \leq E \leq 1500 \text{ keV} \\ \frac{1}{1 + 1.7 \times 10^{-13} V^6} \sum_{n=1}^7 \bar{A}_n V^n, & 1500 < E \leq 10^5 \text{ keV}, \end{cases} \quad (4)$$

where

$$\bar{C} = \sum_{i=1}^N f_i C^i \quad (5)$$

and

$$\bar{A}_n = \sum_{i=1}^N f_i A_n^i \quad (6)$$

We have used superscripts on the fitting parameters to designate the element, and  $V$  has the same meaning here as it did in Eq. (1). Therefore, the approximation for a composite material reduces to the same form as that of a single element, and the fitting parameters for the composite material are obtained simply by averaging the ones for the constituent elements.

#### REFERENCES

1. F. Biggs and R. Lighthill, Analytical Approximations for X-Ray Cross Sections, SC-RR-66-452, Sandia Laboratories, Albuquerque, New Mexico, 1967.
2. F. Biggs, A Generalized Rational Function Least-Squares Fitting Technique, SC-RR-66-2601, Sandia Laboratories, Albuquerque, New Mexico, 1967.
3. Ellery Storm and Harvey I. Israel, Photon Cross Sections From 0.001 to 100 MeV for Elements 1 through 100, LA-3753 (UC-34 Physics, TID-4500), Los Alamos Scientific Laboratory, June 1967 (distributed November 15, 1967).

TABLE I APPROXIMATION PARAMETERS

Z	EL	RMS ERROR	C	A(1)	A(2)	A(3)	A(4)	A(5)	A(6)	A(7)
1	N	1.02*002	1.150*010	-5.550*007	-9.100*008	9.820*009	-9.700*011	2.770*013	4.500*016	1.640*018
2	NE	6.31*003	1.169*010	1.617*006	-3.188*007	1.860*008	-2.524*010	1.488*012	-3.750*015	6.060*018
3	LI	2.13*002	1.526*010	4.590*006	-6.320*007	3.060*008	-4.151*010	2.472*012	-6.385*015	9.000*018
4	BE	1.78*002	2.060*010	-5.080*006	1.910*007	8.770*009	-1.194*010	4.940*013	-9.000*017	2.350*018
5	B	1.68*002	2.707*010	4.160*006	-7.530*007	4.310*008	-5.970*010	3.560*012	-9.100*015	1.320*017
6	C	8.70*003	3.472*010	2.500*007	-5.217*007	4.260*008	-6.093*010	3.650*012	-9.150*015	1.410*017
7	N	-2.34*002	3.999*010	-1.370*005	6.940*007	8.500*009	-1.410*010	4.900*013	9.500*016	2.900*018
8	O	1.23*002	4.600*010	1.274*006	-7.757*007	5.898*008	-8.410*010	5.035*012	-1.265*014	1.890*017
9	F	1.45*002	4.921*010	-7.920*006	9.300*008	3.450*008	-4.940*010	2.520*012	-4.700*015	9.500*018
10	NE	1.28*002	5.748*010	2.287*006	-1.034*006	7.598*008	-1.093*009	6.623*012	-1.696*014	2.470*017
11	NA	1.54*002	6.143*010	-1.226*005	2.880*007	3.627*008	-5.330*010	2.795*012	-4.650*015	1.040*017
12	M3	1.40*002	6.961*010	1.154*006	-1.090*006	8.668*008	-1.256*009	7.610*012	-1.940*014	2.834*017
13	A	1.62*002	7.336*010	5.930*006	-1.598*006	1.059*007	-1.528*009	9.374*012	-2.460*014	3.460*017
14	SI	1.21*002	8.213*010	-5.460*006	-6.530*007	8.240*008	-1.267*009	7.130*012	-1.700*014	2.614*017
15	P	2.20*002	8.715*010	1.190*005	-2.250*006	1.329*007	-1.871*009	1.123*011	-2.873*014	3.920*017
16	S	1.26*002	9.452*010	-2.060*006	-1.138*006	1.068*007	-1.554*009	9.270*012	-2.271*014	3.340*017
17	CL	2.78*002	9.816*010	2.400*005	-3.560*006	1.840*007	-2.618*009	1.625*011	-4.410*014	5.800*017
18	A	1.20*002	9.733*010	-1.050*005	-3.700*007	8.440*008	-1.264*009	7.495*012	-1.770*014	2.810*017
19	K	4.82*003	1.110*007	-3.800*006	-1.177*006	1.200*007	-1.776*009	1.390*011	-2.730*014	4.830*017
20	CA	1.68*002	1.205*007	6.256*006	-2.166*006	1.548*007	-2.217*009	1.330*011	-3.350*014	4.700*017
21	SC	1.69*002	1.180*007	-2.459*005	6.906*007	6.507*008	-1.006*009	5.560*012	-1.070*014	2.100*017
22	TI	1.48*002	1.217*007	-2.057*005	2.830*007	8.000*008	-1.208*009	6.770*012	-1.363*014	2.440*017
23	V	1.63*002	1.275*007	1.075*005	-2.700*006	1.787*007	-2.615*009	1.633*011	-4.400*014	6.100*017
24	Q2	1.90*002	1.377*007	2.018*005	-3.610*006	2.111*007	-3.038*009	1.883*011	-3.060*014	5.830*017
25	W	1.91*002	1.416*007	3.600*006	-2.130*006	1.674*007	-2.435*009	1.479*011	-3.780*014	5.370*017
26	FE	1.22*002	1.508*007	-6.900*006	-1.309*006	1.900*007	-2.230*009	1.358*011	-3.410*014	2.130*017
27	CO	1.67*002	1.550*007	5.000*006	-2.458*006	1.892*007	-2.790*009	1.724*011	-4.515*014	6.300*017
28	NI	1.56*002	1.677*007	-3.566*005	1.128*006	8.674*008	-1.410*009	8.220*012	-1.730*014	3.260*017
29	CU	1.44*002	1.872*007	-3.230*005	8.500*007	9.570*008	-1.539*009	9.342*012	-1.965*014	3.464*017
30	ZN	1.32*002	1.765*007	-3.000*005	5.700*007	1.879*007	-1.700*009	1.000*011	-2.230*014	3.840*017
31	GA	1.27*002	1.778*007	-2.533*005	9.000*008	1.255*007	-1.981*009	1.210*011	-2.940*014	4.700*017
32	GE	1.48*002	1.813*007	-4.167*005	1.513*006	9.500*008	-1.460*009	8.770*012	-1.920*014	3.560*017
33	AS	1.64*002	1.889*007	-4.449*005	1.749*006	8.007*008	-1.385*009	8.070*012	-1.630*014	3.200*017
34	SE	1.37*002	1.932*007	-1.380*005	-1.457*006	1.807*007	-2.074*009	1.310*011	-4.810*014	6.970*017
35	BR	2.44*002	2.019*007	-8.280*005	5.100*006	-1.260*006	-1.600*010	2.200*013	7.700*015	5.600*018
36	AD	1.88*002	2.857*007	-4.678*005	1.730*006	9.572*008	-1.682*009	1.041*011	-2.417*014	4.300*017
37	MB	1.80*002	2.151*007	-3.382*005	5.200*007	1.300*007	-2.283*009	1.350*011	-3.250*014	5.200*017
38	SA	1.93*002	2.228*007	-4.930*005	1.855*006	1.003*007	-1.743*009	1.054*011	-2.320*014	4.170*017
39	V	2.38*002	2.325*007	-9.670*005	8.080*006	-2.310*008	-9.000*011	-2.190*013	9.800*015	4.500*018
40	ZY	1.48*002	2.428*007	-3.770*005	6.700*007	1.470*007	-2.394*009	1.464*011	-3.470*014	5.500*017

(continued on next page)

TABLE I (Cont)

Z	E <sub>z</sub>	RMS ERROR	C	A(1)	A(2)	A(3)	A(4)	A(5)	A(6)	A(7)
41	NB	1.66*002	2.559*007	-2,280*005	-6,760*007	1,912*007	-2,964*009	1,800*011	-4,380*014	6,500*017
42	MD	1.86*002	2.594*007	-8,510*005	4,390*006	2,710*008	-8,350*010	4,800*012	-5,400*015	2,360*017
43	TC	1.48*002	2.678*007	-4,760*005	1,470*006	1,342*007	-2,270*009	1,390*011	-3,230*014	5,370*017
44	RJ	1.71*002	2.789*007	-5,870*005	2,480*006	1,063*007	-1,876*009	1,108*011	-2,270*014	4,200*017
45	RM	2.20*002	2.851*007	-1,112*004	7,220*006	-3,570*008	4,600*011	-1,530*012	1,640*014	-2,700*018
46	PD	2.56*002	3.002*007	1,813*005	-4,576*006	3,318*007	-4,984*009	3,148*011	-8,520*014	1,150*016
47	AG	1.80*002	3.082*007	-4,230*005	8,800*007	1,680*007	-2,738*009	1,645*011	-3,750*014	5,900*017
48	CD	1.80*002	3.095*007	-9,240*005	5,397*006	3,320*008	-9,960*010	5,770*012	-6,900*015	2,540*017
49	IV	1.53*002	3.204*007	-4,900*005	1,370*006	1,630*007	-2,794*009	1,760*011	-4,320*014	6,800*017
50	SV	1.86*002	3.277*007	-2,640*005	-6,200*007	2,253*007	-3,580*009	2,259*011	-5,844*014	8,600*017
51	SD	1.86*002	3.386*007	-1,170*005	-1,980*006	2,698*007	-4,250*009	2,702*011	-7,160*014	1,006*016
52	TC	1.32*002	3.349*007	-5,680*005	2,110*006	1,450*007	-2,809*009	1,673*011	-4,147*014	6,705*017
53	I	1.38*002	3.517*007	-9,180*005	5,170*006	6,110*008	-1,505*009	9,570*012	-1,940*014	4,300*017
54	XE	2.21*002	3.553*007	-1,440*004	9,920*006	-8,250*008	4,000*010	-2,550*012	1,660*014	3,100*018
55	CS	2.92*002	3.656*007	-1,790*004	1,295*005	-1,655*007	1,440*009	-8,900*012	3,514*014	-1,680*017
56	BA	2.54*002	3.717*007	-1,670*004	1,197*005	-1,384*007	1,130*009	-7,300*012	3,160*014	-1,400*017
57	LS	2.69*002	3.838*007	-1,940*004	1,338*005	-1,720*007	1,510*009	-9,500*012	3,800*014	-2,100*017
58	CE	2.73*002	3.983*007	-1,952*004	1,442*005	-2,006*007	1,918*009	-1,243*011	4,800*014	-3,300*017
59	PR	3.01*002	4.152*007	-2,150*004	1,613*005	-2,434*007	2,423*009	-1,540*011	3,664*014	-4,150*017
60	ND	1.51*002	4.281*007	-1,280*004	8,360*006	-8,200*009	-6,730*010	4,020*012	-4,000*016	2,200*017
61	PM	1.54*002	4.469*007	-9,660*005	5,460*006	8,800*008	-2,000*009	1,266*011	-2,650*014	5,200*017
62	SM	1.48*002	4.513*007	-1,074*004	6,500*006	5,600*008	-1,580*009	1,000*011	-1,843*014	4,270*017
63	EJ	1.48*002	4.635*007	-1,373*004	9,130*006	-1,700*008	-6,375*010	4,027*012	-3,000*016	2,300*017
64	GD	1.44*002	4.663*007	-1,503*004	1,040*005	-5,760*008	-9,500*011	5,700*013	9,900*015	1,100*017
65	TS	1.77*002	4.765*007	-1,906*004	1,393*005	-1,572*007	1,207*009	-7,900*012	3,650*014	-2,000*017
66	DY	1.33*002	4.900*007	-1,400*004	9,360*006	-1,400*008	-7,530*010	5,000*012	-3,600*015	2,700*017
67	MD	1.44*002	4.956*007	-1,692*004	1,194*005	-8,770*008	1,900*010	-8,200*013	1,340*014	9,000*018
68	ER	1.68*002	5.079*007	-1,931*004	1,399*005	-1,410*007	8,260*010	-4,560*012	2,400*014	-2,000*018
69	TM	1.55*002	5.251*007	-2,001*004	1,466*005	-1,573*007	1,045*009	-6,200*012	2,994*014	-9,000*018
70	YB	1.27*002	5.366*007	-1,830*004	1,317*005	-1,105*007	4,200*010	-2,290*012	1,870*014	3,000*018
71	LJ	1.25*002	5.478*007	-2,000*004	1,457*005	-1,430*007	7,460*010	-3,700*012	2,100*014	3,000*018
72	MF	1.08*002	5.634*007	-1,212*004	7,540*006	7,170*008	-2,130*009	1,483*011	-3,510*014	6,700*017
73	TA	1.03*002	5.709*007	-1,836*004	1,313*005	-9,300*008	4,000*011	8,400*013	7,800*015	1,800*017
74	M	9.96*003	5.860*007	-1,870*004	1,330*005	-8,700*008	1,500*010	2,640*012	1,050*015	2,700*017
75	RE	1.18*002	5.962*007	-2,076*004	1,510*005	-1,350*007	4,200*010	-6,000*013	9,770*015	1,270*017
76	OS	1.00*002	6.069*007	-2,020*004	1,462*005	-1,176*007	1,640*010	1,140*012	4,200*015	2,500*017
77	IA	1.32*002	6.291*007	-1,535*004	1,043*005	8,000*009	-1,430*009	1,066*011	-2,210*014	5,300*017
78	PT	1.11*002	6.317*007	-2,485*004	1,882*005	-2,370*007	1,750*009	-9,370*012	3,750*014	-1,360*017
79	AJ	1.33*002	6.511*007	-2,692*004	2,068*005	-2,860*007	2,350*009	-1,300*011	4,810*014	-2,500*017
80	HG	1.08*002	6.651*007	-2,709*004	2,096*005	-2,947*007	2,485*009	-1,403*011	5,190*014	-3,000*017

(continued on next page)

TABLE I (Cont)

Z EL	HMS ERROR	C	A(1)	A(2)	A(3)	A(4)	A(5)	A(6)	A(7)
81 TL	1.25*002	6.723-009	-2,788-004	2,158-005	-3,064-007	2,550-009	-1,393-011	5,020-014	-2,600-017
82 PJ	1.15*002	6.962-009	-2,320-004	1,750-005	-1,800-007	8,360-010	-2,740-012	1,570-014	1,400-017
83 BI	1.07*002	7.115-009	-2,680-004	2,066-005	-2,675-007	1,945-009	-9,722-012	3,690-014	-1,000-017
84 PD	9.27*003	7.342-009	-2,680-004	2,065-005	-2,580-007	1,750-009	-8,190-012	3,165-014	-2,000-018
85 AT	7.78*003	7.572-009	-2,880-004	2,249-005	-3,083-007	2,444-009	-1,304-011	4,820-014	-2,300-017
86 NV	7.64*003	7.426-009	-2,870-004	2,258-005	-3,210-007	2,610-009	-1,377-011	4,880-014	-2,300-017
87 FK	9.87*003	7.560-009	-3,300-004	2,628-005	-4,214-007	3,872-009	-2,168-011	7,290-014	-5,022-017
88 RA	9.10*003	7.809-009	-2,900-004	2,290-005	-3,194-007	2,523-009	-1,306-011	4,670-014	-1,940-017
89 AC	1.02*002	8.012-009	-2,750-004	2,146-005	-2,650-007	1,700-009	-7,398-012	2,900-014	2,000-018
90 TH	9.40*003	8.143-009	-2,940-004	2,334-005	-3,240-007	2,530-009	-1,307-011	4,750-014	-2,200-017
91 PA	8.40*003	8.446-009	-3,190-004	2,562-005	-3,830-007	3,240-009	-1,730-011	5,960-014	-3,300-017
92 U	1.11*002	8.415-009	-2,960-004	2,360-005	-3,250-007	2,430-009	-1,200-011	4,310-014	-1,500-017
93 NP	1.58*002	8.754-009	-2,660-004	2,080-005	-2,250-007	1,037-009	-2,760-012	1,490-014	1,850-017
94 PJ	1.45*002	8.907-009	-2,660-004	2,105-005	-2,360-007	1,190-009	-3,750-012	1,600-014	1,500-017
95 AN	9.05*003	9.153-009	-3,340-004	2,700-005	-3,990-007	3,201-009	-1,594-011	5,334-014	-2,360-017
96 CA	8.39*003	9.270-009	-3,720-004	3,046-005	-5,000-007	4,501-009	-2,406-011	7,750-014	-5,100-017
97 BK	8.43*003	9.454-009	-3,480-004	2,837-005	-4,340-007	3,630-009	-1,960-011	6,160-014	-3,300-017
98 CF	1.39*002	9.789-009	-3,250-004	2,657-005	-3,787-007	2,913-009	-1,430-011	4,962-014	-2,000-017
99 ED	1.28*002	9.931-009	-3,330-004	2,718-005	-3,870-007	2,910-009	-1,360-011	4,560-014	-1,300-017
100 FH	9.99*003	1.022-008	-3,810-004	3,140-005	-5,000-007	4,307-009	-2,215-011	7,100-014	-4,107-017



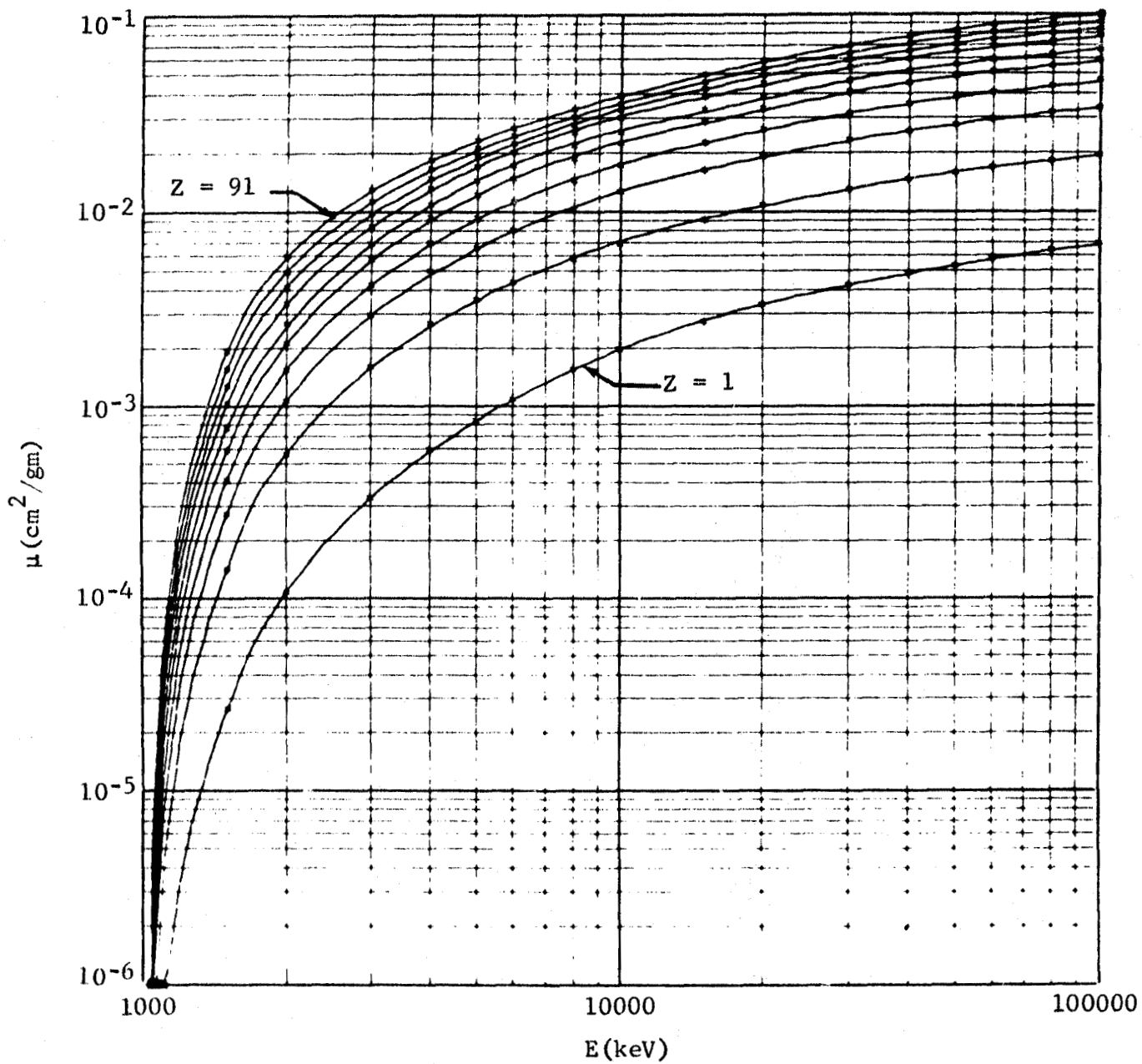


Fig. 1 Pair-production cross section as a function of energy for the elements with atomic numbers  $Z = 1, 11, 21, 31, 41, 51, 61, 71, 81, 91$ . Cross sections increase monotonically with atomic numbers.

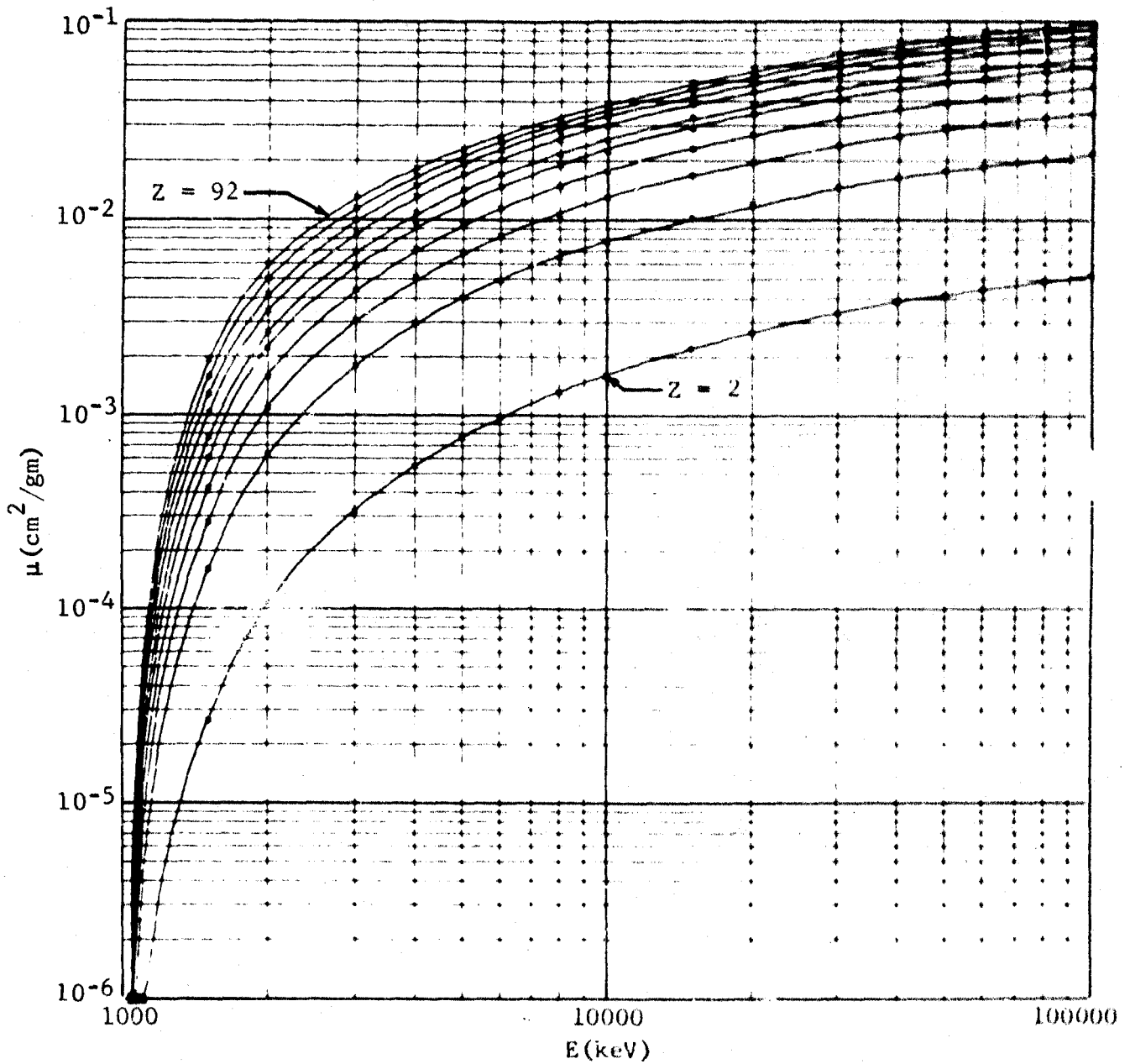


Fig. 2 Pair-production cross section as a function of energy for the elements with atomic numbers  $Z = 2, 12, 22, 32, 42, 52, 62, 72, 82, 92$ . Cross sections increase monotonically with atomic numbers.

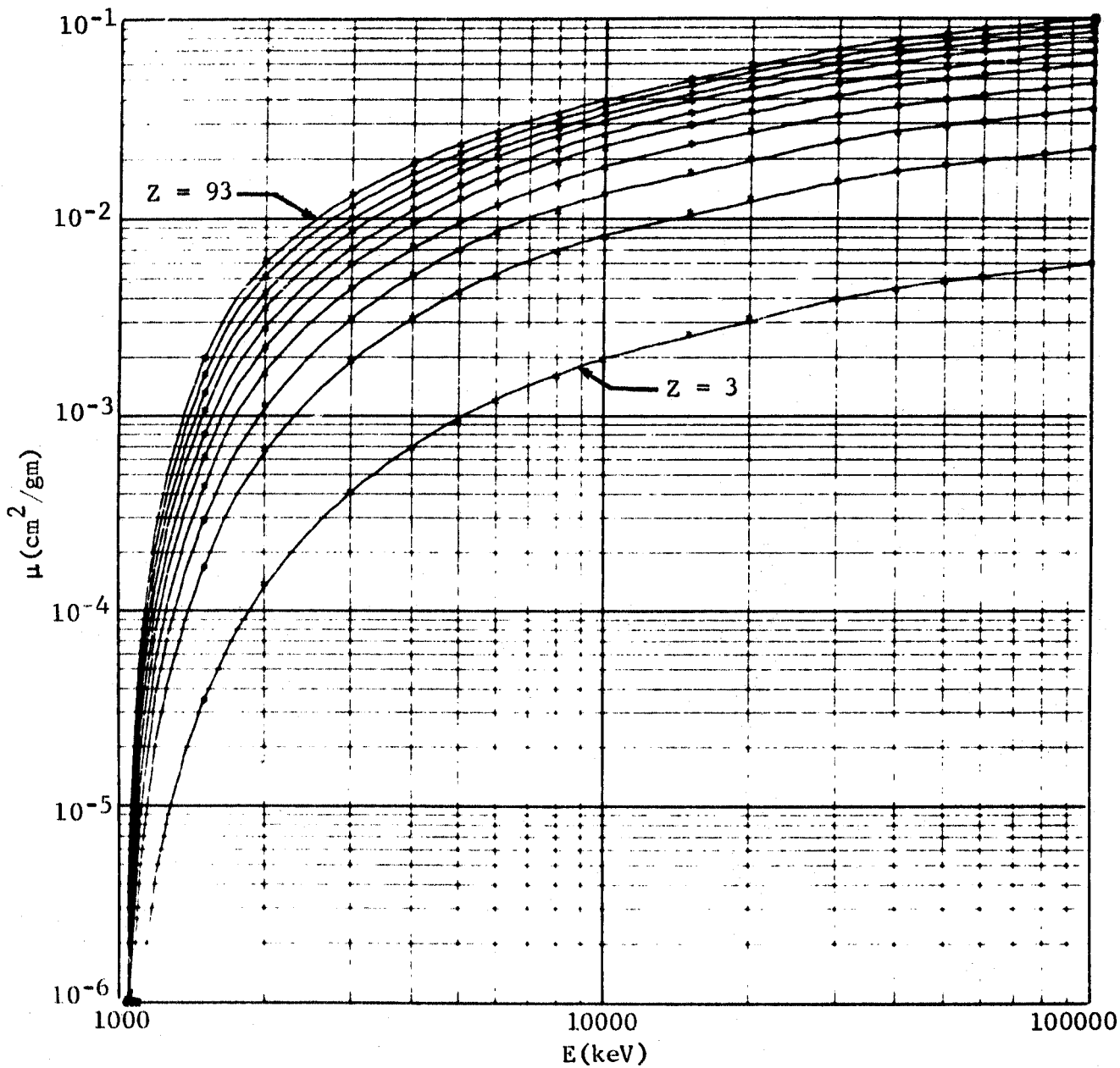


Fig. 3 Pair-production cross section as a function of energy for the elements with atomic numbers  $Z = 3, 13, 23, 33, 43, 53, 63, 73, 83, 93$ . Cross sections increase monotonically with atomic numbers.

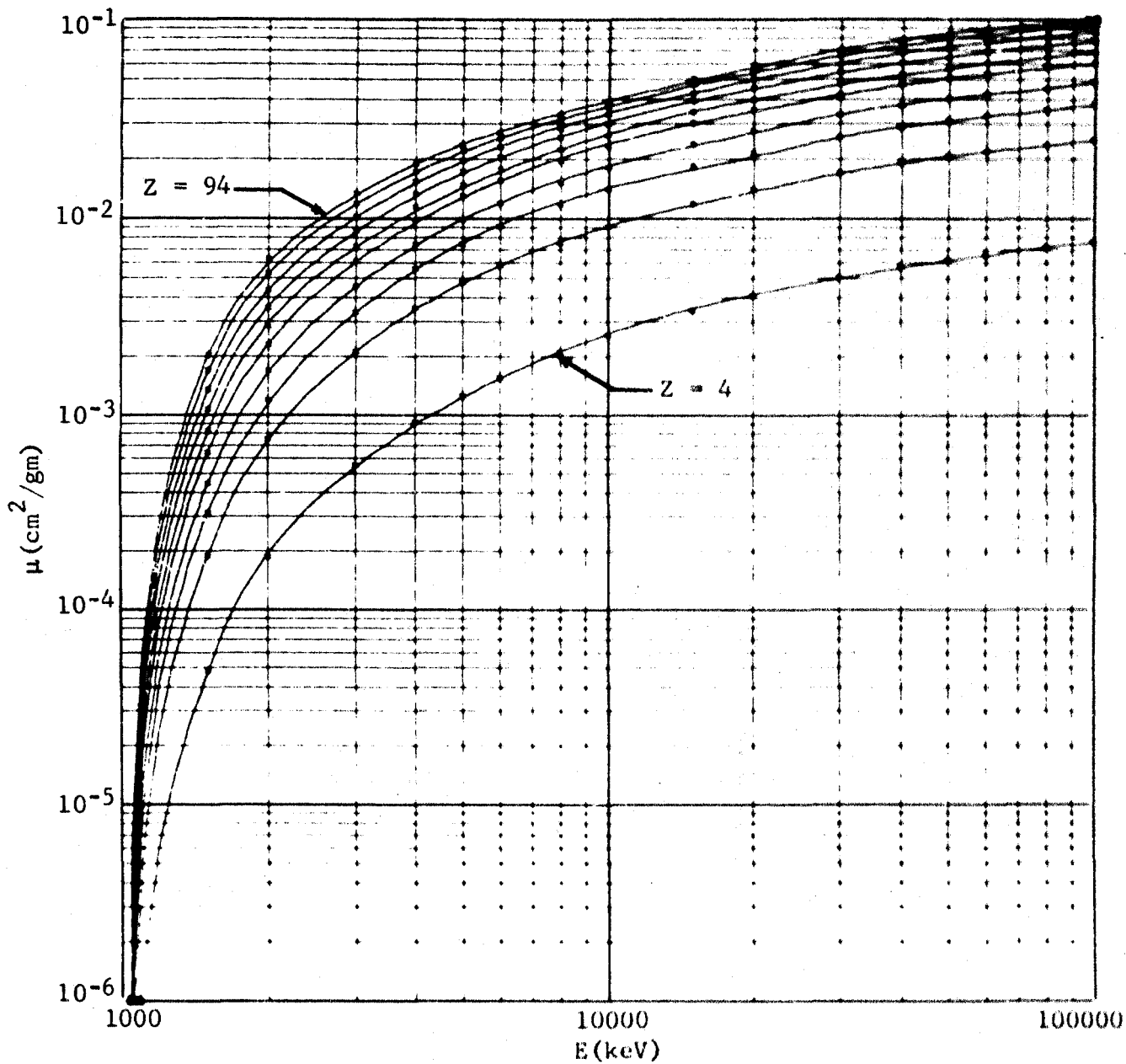


Fig. 4 Pair-production cross section as a function of energy for the elements with atomic numbers  $Z = 4, 14, 24, 34, 44, 54, 64, 74, 84, 94$ . Cross sections increase monotonically with atomic numbers.

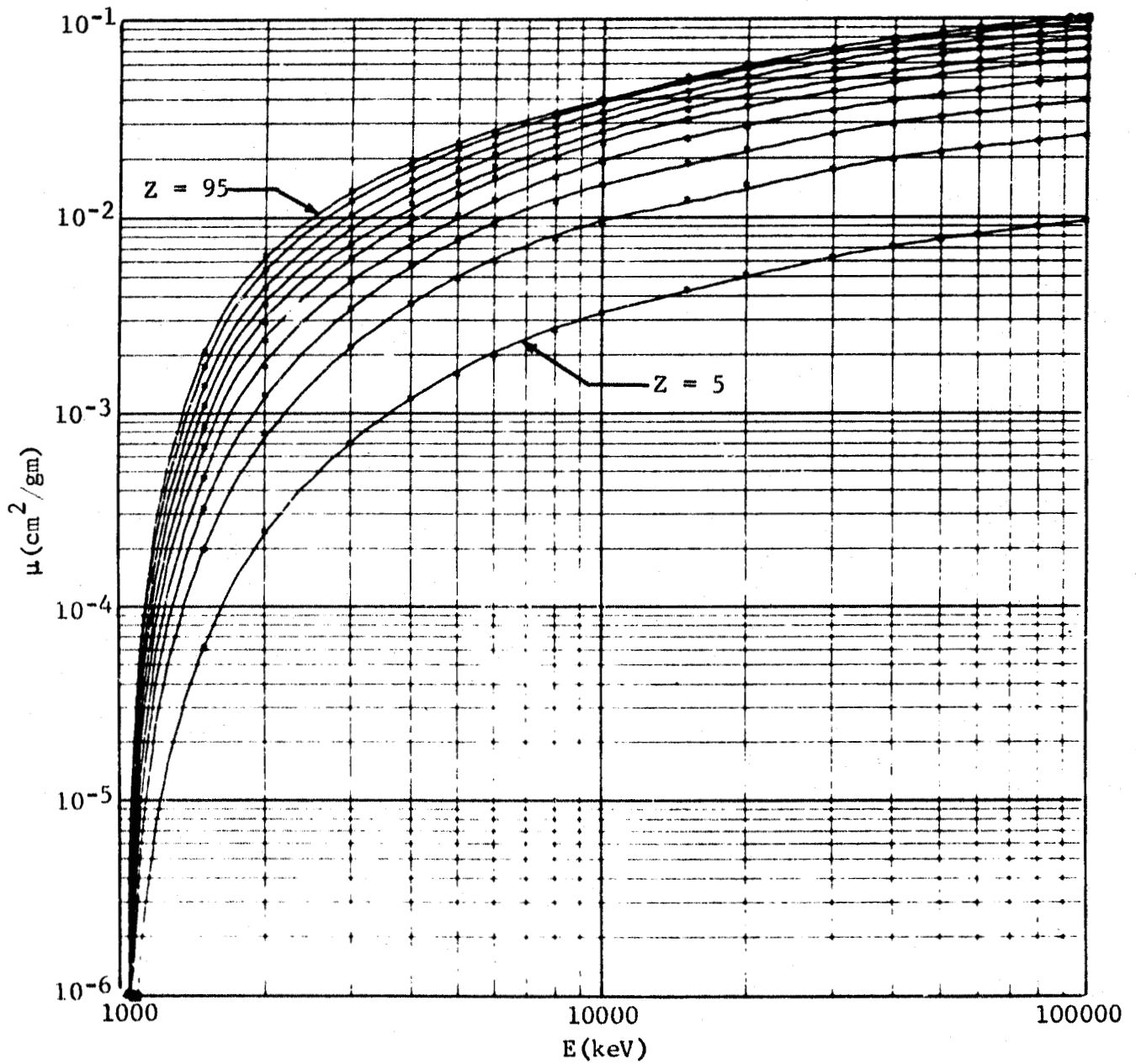


Fig. 5 Pair-production cross section as a function of energy for the elements with atomic numbers  $Z = 5, 15, 25, 35, 45, 55, 65, 75, 85, 95$ . Cross sections increase monotonically with atomic numbers.

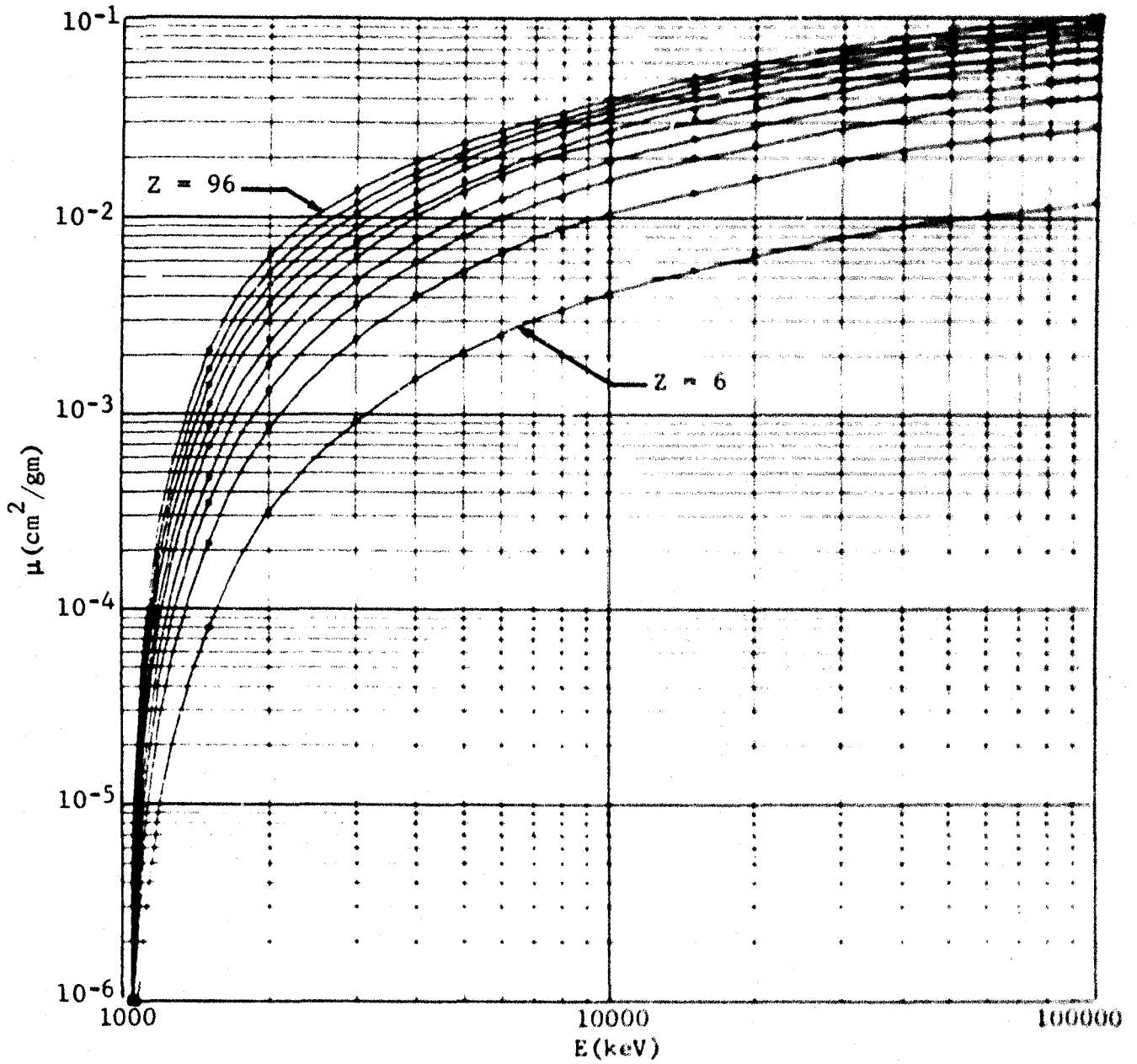


Fig. 6 Pair-production cross section as a function of energy for the elements with atomic numbers  $Z = 6, 16, 26, 36, 46, 56, 66, 76, 86, 96$ . Cross sections increase monotonically with atomic numbers.

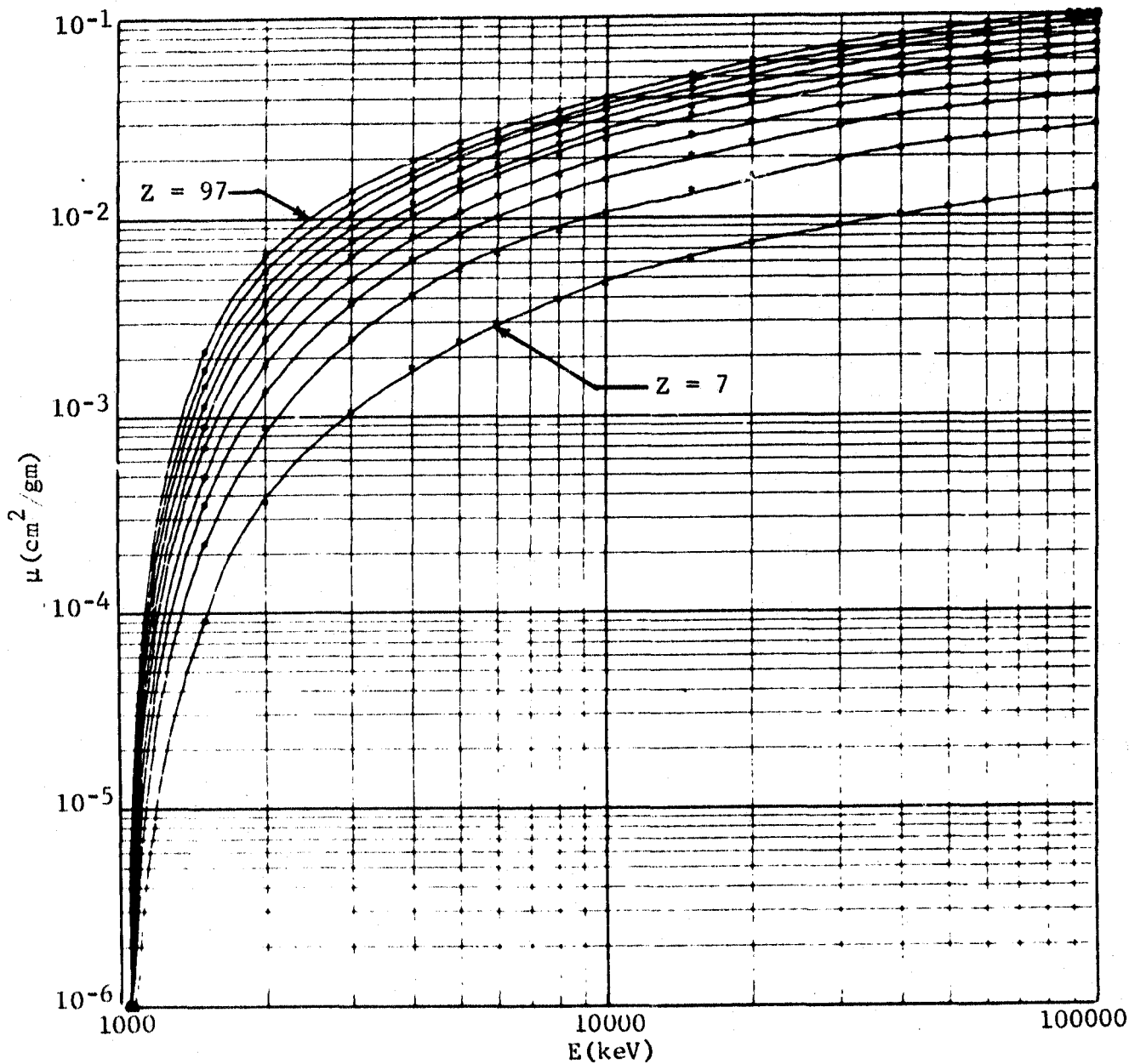


Fig. 7 Pair-production cross section as a function of energy for the elements with atomic numbers  $Z = 7, 17, 27, 37, 47, 57, 67, 77, 87, 97$ . Cross sections increase monotonically with atomic numbers.

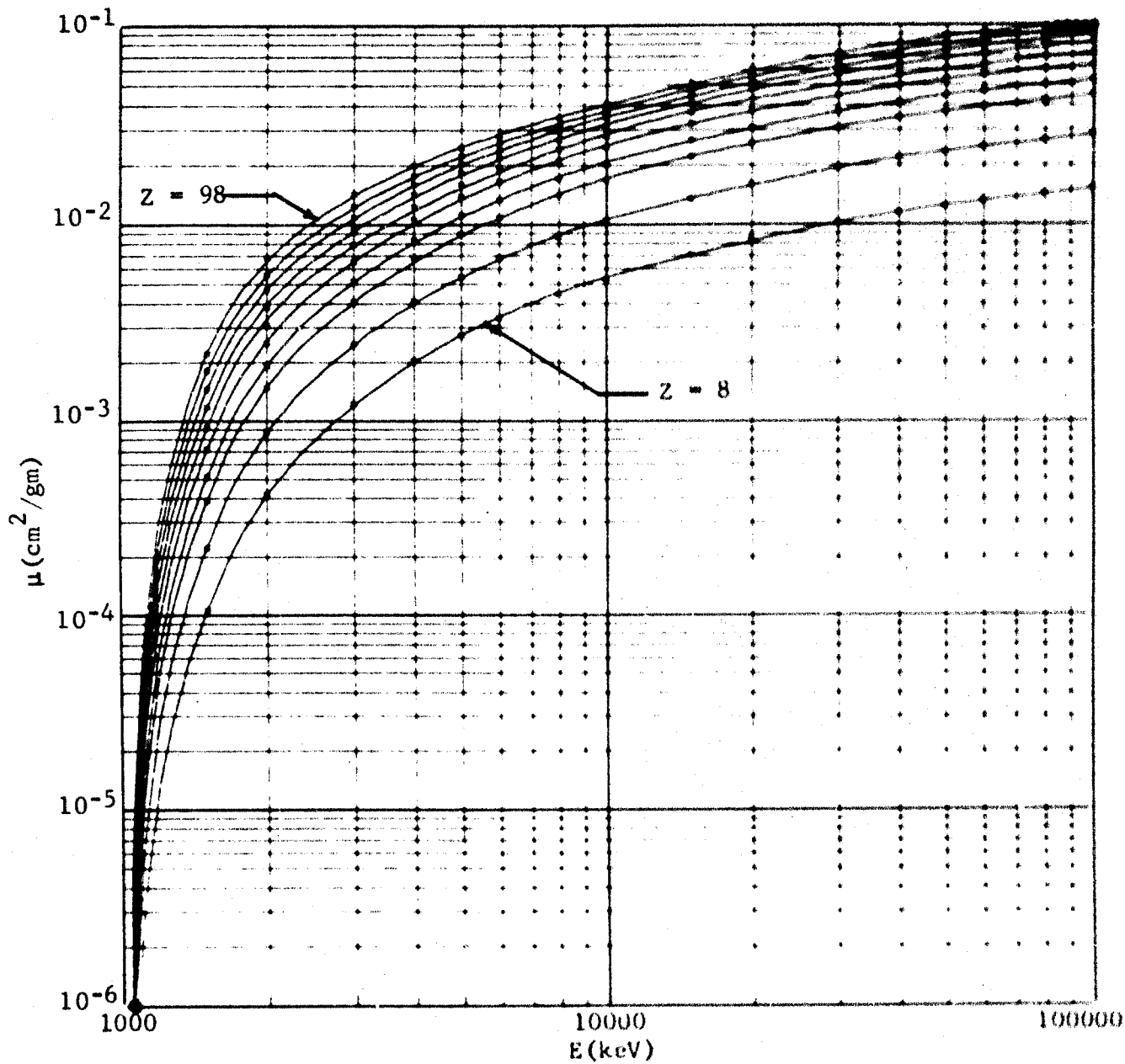


Fig. 8 Pair-production cross section as a function of energy for the elements with atomic numbers  $Z = 8, 18, 28, 38, 48, 58, 68, 78, 88, 98$ . Cross sections increase monotonically with atomic numbers.



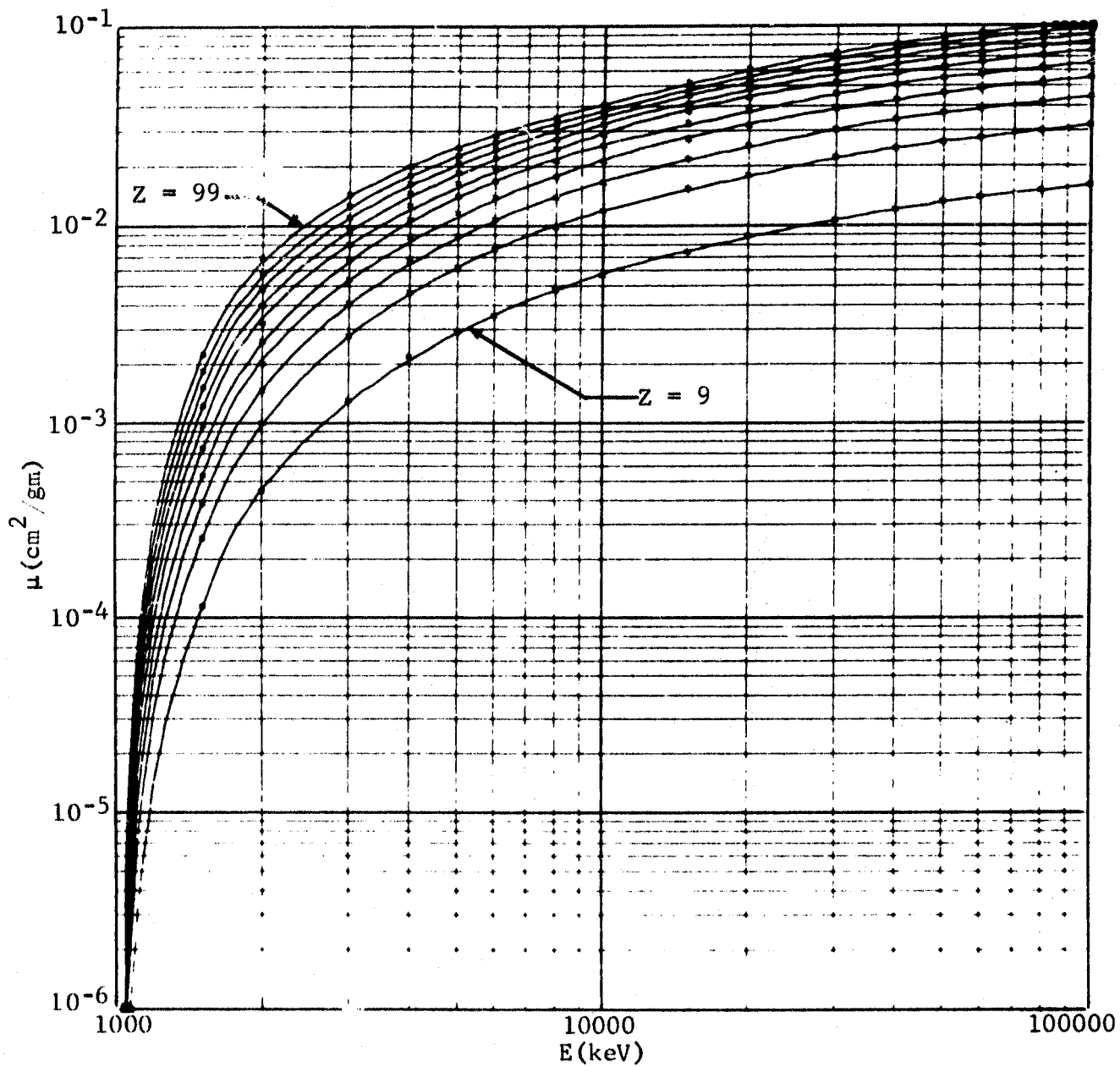


Fig. 9 Pair-production cross section as a function of energy for the elements with atomic numbers  $Z = 9, 19, 29, 39, 49, 59, 69, 79, 89, 99$ . Cross sections increase monotonically with atomic numbers.

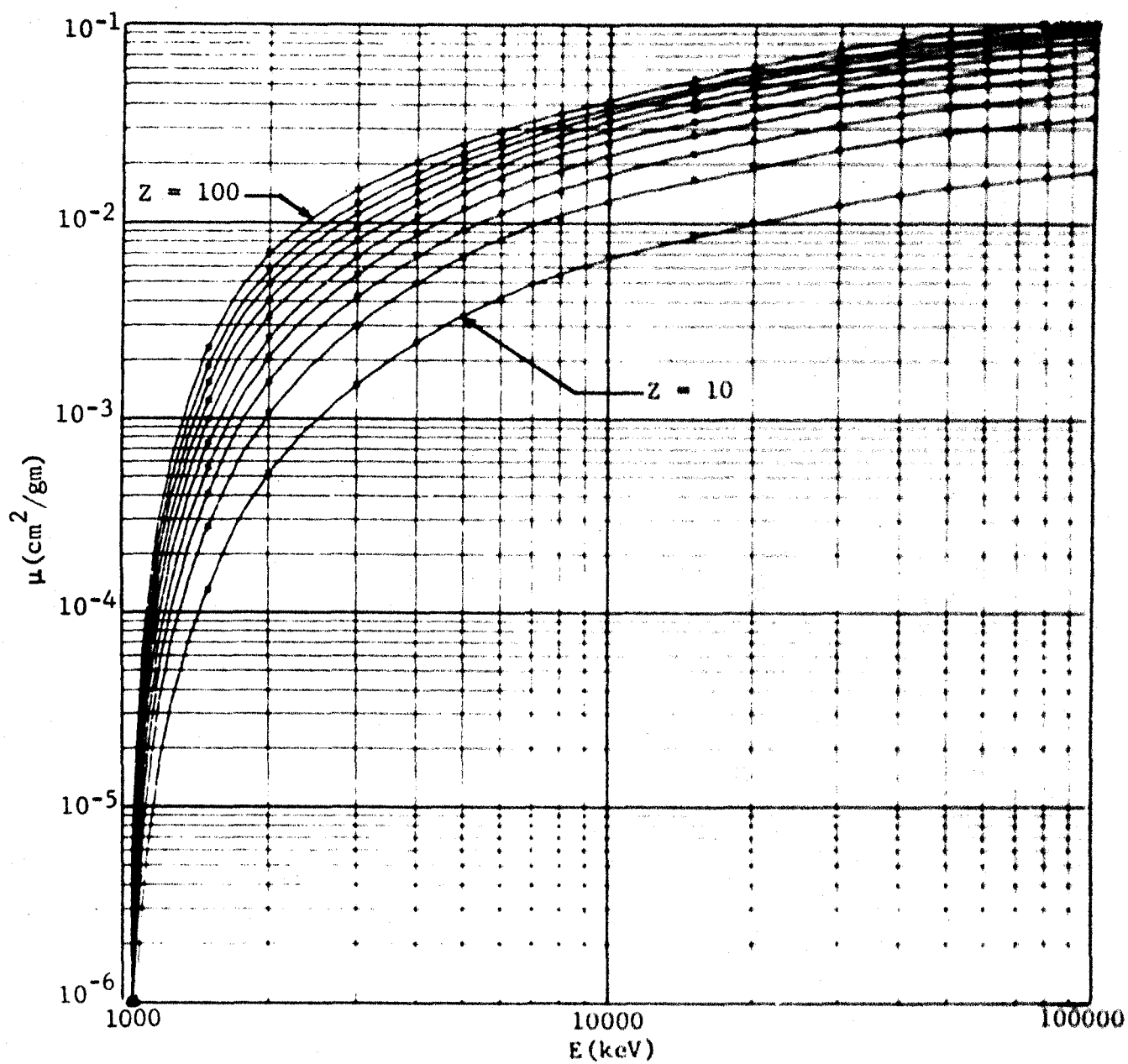


Fig. 10 Pair-production cross section as a function of energy for the elements with atomic numbers  $Z = 10, 20, 30, 40, 50, 60, 70, 80, 90, 100$ . Cross sections increase monotonically with atomic numbers.

**DISTRIBUTION:**

N. A. Beauchamp  
Bell Telephone Laboratories  
Whippany, New Jersey

R. D. Evans  
Massachusetts Institute of  
Technology  
Cambridge, Massachusetts

J. Marcum  
Rand Corporation  
1700 Main St.  
Santa Monica, California

Director, Air Force Weapons  
Laboratory  
Kirtland AFB, New Mexico 87117  
Attn: Maj. Robert H. Hansen (1)  
Lt. R. J. Cahill (1)

Maj. Loren C. Logie  
Hq., DASA  
Washington, D.C.

Dr. Allan Bearden  
University of California  
Department of Chemistry  
LaJolla, California 92038

Mr. Laverne Birks  
U.S. Naval Research Laboratory  
Washington, D.C. 20390

Mr. Warren Chan  
General Electric Company  
DASA Information & Analysis Center  
816 State St.  
Santa Barbara, California 93101

Dr. Kurt Heinrich, Director  
National Bureau of Standards  
Washington, D.C. 20234

Dr. Charles Francis  
Aerospace Corporation  
111 E. Mill Street  
San Bernardino, California 92408

Dr. Burton L. Henke  
Department of Physics and Astronomy  
University of Hawaii  
Honolulu, Hawaii 96822

Mr. John H. Hubbell, Director  
National Bureau of Standards  
Radiation Theory Section  
Washington, D.C. 20234

Mrs. Nancy Kerr Della-Grande  
University of California  
Lawrence Radiation Laboratory  
P.O. Box 808  
Livermore, California 94551

University of California  
Lawrence Radiation Laboratory  
P.O. Box 808  
Livermore, California 94551  
Attn: Technical Information Div.  
For: Dr. William H. McMaster (1)  
Dr. Charles J. Taylor (1)  
Dr. James C. Watson (1)

Los Alamos Scientific Laboratory  
P.O. Box 1663  
Los Alamos, New Mexico 87544  
Attn: Dr. James H. McCrary (1)  
Dr. John A. Northrup (1)  
Dr. Laura J. Shreffler (1)  
Dr. Elizabeth Plassmann (1)  
Dr. Henry Sandmeier (1)  
Dr. Jerry Conner (1)

Dr. Wm. Veigele  
Kaman Nuclear  
Division of Kaman Aircraft Corp.  
Garden of the Gods Road  
Colorado Springs, Colorado 80907

Dr. Clayton Zerby  
Union Carbide Corporation  
Electronics Division  
Santa Monica, California

Peter H. Haas, Assistant to  
DDST for Experimental Research  
Hq/DASA  
Washington, D.C.

Dr. Sterling Colgate  
New Mexico Institute of Mining  
and Technology  
Department of Physics  
Socorro, New Mexico

Dr. G. T. Clayton  
University of Arkansas  
Department of Physics  
Fayetteville, Arkansas

Thomas Dolce  
Ballistic Research Laboratory  
Aberdeen Proving Ground  
Aberdeen, Maryland

DISTRIBUTION (Cont):

D. G. Abshier  
North American Rockwell  
Autonetics Division  
3370 Miraloma Avenue  
Anaheim, California

Lockheed Missiles and Space Co.  
Sunnyvale, California 94088  
Attn: Mr. G. Dunbar (1)  
Mr. Vernon Field (1)

W. L. Bade  
Avco Space Systems Division  
Wilmington, Massachusetts 01887

R. S. Overhotsky  
Moleculon Research Corp.  
139 Main St.  
Cambridge, Massachusetts

Jane Z. Frazer  
Department of Earth Sciences  
University of California  
LaJolla, California 92037

R. C. Willis  
Martin-Marietta Corp.  
Denver, Colorado 80201

L. E. Preuss  
Department of Physics  
Edsel B. Ford Institute for  
Medical Research  
2799 West Grand Boulevard  
Detroit, Michigan 48202

D. B. Shuster, 1200  
W. C. Myre, 1210  
J. C. Wardlow, 1211  
R. G. Fitzgerald, 1221  
T. W. Hoover, 1222  
H. M. Stoller, 1222  
R. L. Alvis, 1222  
G. V. Barton, 1222  
J. L. Irwin, 1222  
W. J. Roh, 1222  
J. M. Manweller, 1222  
J. J. Lang, 1223  
A. J. Chabai, 1224  
D. B. Hayes, 1224  
N. C. Anderholm, 1224  
L. Dehghanmanesh, 1224  
H. S. Lauson, 1224  
L. Kennedy, 1224  
J. R. Piper, 1224  
J. N. Middleton, 1516  
T. B. Lane, 1540  
D. M. Ellett, 1541  
W. A. Sebrell, 1542  
L. J. Johnson, 1545

L. K. Johnson, 1545  
C. W. Moses, 1548  
E. M. Austin, 1548  
L. G. Rainhart, 1548  
W. H. Schmidt, 1548  
P. P. Stirbis, 1548  
J. W. Weihe, 1710  
R. G. Clem, 1730  
Deanna Rawlinson, 1731  
D. Snyder, 1731  
G. S. Bennett, 1811  
R. W. Corwin, 1820  
W. C. Lyons, 1820  
C. C. Hudson, 1830  
L. D. Smith, 2300  
C. G. Scott, 2316  
F. B. Brumley, 2316  
A. W. Battaglia, 2316  
W. D. Lacoss, 2611  
F. N. Coppage, 2613  
M. P. Salomon, 2613  
J. A. Cooper, 2625  
F. L. Chavez, 2625  
J. L. Duncan, 2635  
S. J. Buchsbaum, 5000  
A. Narath, 5100  
G. W. Gobell, 5110  
B. Morosin, 5131  
D. C. Wallace, 5151  
W. Herrmann, 5160  
B. M. Butcher, 5161  
F. R. Tuler, 5161  
C. H. Karnes, 5162  
L. D. Bertholf, 5162  
R. J. Lawrence, 5162  
L. G. Lee, 5162  
E. Young, 5162  
D. E. Munson, 5163  
L. C. Hebel, 5200  
C. R. Mehl, 5230  
K. G. Adams, 5231  
F. Biggs, 5231 (5)  
D. A. Dahlgren, 5231  
R. Lighthill, 5231 (3)  
D. J. McCloskey, 5231  
R. Cole, 5231  
J. H. Renken, 5231  
S. L. Thompson, 5231  
G. W. McClure, 5232  
J. M. Hoffman, 5233  
C. N. Vittitoe, 5233  
G. L. Cano, 5235  
R. W. Harris, 5235  
G. H. Miller, 5235  
F. W. Neilson, 5240  
E. H. Beckner, 5242  
J. D. Shreve, 5271  
C. F. Bild, 5400  
J. E. McDonald, 5410  
R. K. Traeger, 5411

DISTRIBUTION (Cont):

D. R. Anderson, 5411  
M. F. Furney, 5411  
K. D. Smith, 5411  
R. L. LaChance, 5412  
P. J. Thoma, 5413  
W. M. O'Neill, 5420  
E. J. Graeber, 5422  
K. E. Lawson, 5422  
K. E. Mead, 5424  
L. M. Berry, 5430  
C. E. Albright, 5431  
S. A. Moore, 7230  
D. E. Gregson, 8130  
P. H. Lasky, 8133  
E. E. Ives, 8159  
O. Tjeltweed, 8173  
P. D. Gildea, 8174  
C. H. Stoll, 8174  
J. C. King, 8300  
A. N. Blackwell, 8310  
L. H. Bakken, 8314  
J. L. Wirth, 8320  
H. G. Short, 8322  
J. A. Mogford, 8334  
B. F. Murphey, 9100  
C. D. Broyles, 9110  
L. R. Hill, 9111  
M. L. Merritt, 9111  
W. D. Weart, 9111  
J. D. Plimpton, 9112  
J. L. Benson, 9112  
J. V. Walker, 9113  
J. A. Halbleib, 9113  
R. A. Richards, 9121  
W. Cook, 9122  
G. Eggert, 9122  
D. Overmier, 9122  
H. B. Austin, 9124  
D. S. Hill, 9124  
S. A. Ingham, 9125  
D. C. MacMillan, 9125  
R. L. Rutter, 9126  
H. M. Dumas, 9213  
B. F. Blackwell, 9328  
I. Auerbach, 9342  
W. C. McKinley, 9411  
B. F. Hefley, 8232 (5)  
B. R. Allen, 3421  
L. C. Baldwin, 3412  
W. J. Wagoner, 3413  
For: DTIE (3)  
C. H. Sproul, 3428-2 (10)